



Supplement of

Phase transition observations and discrimination of small cloud particles by light polarization in expansion chamber experiments

Leonid Nichman et al.

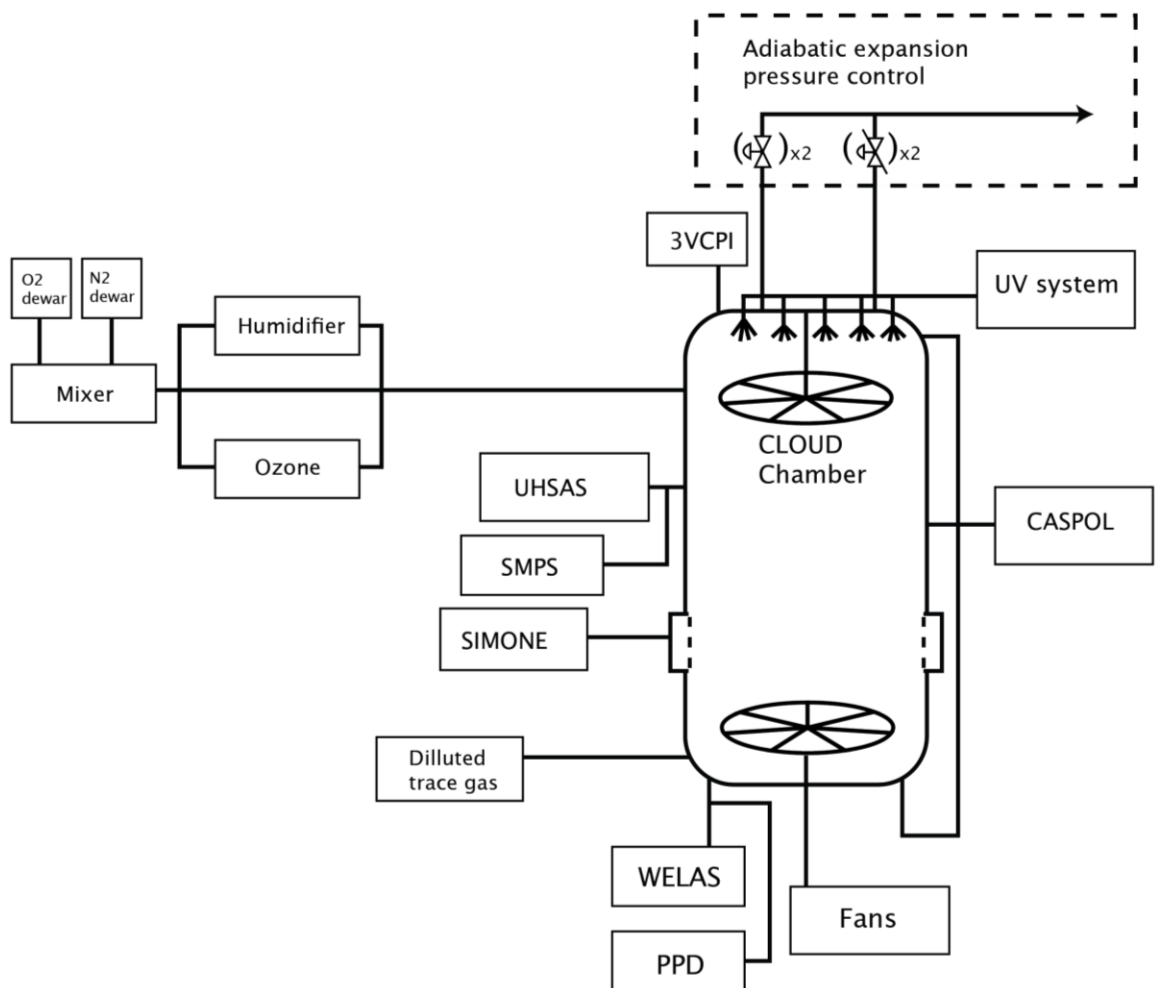
Correspondence to: Leonid Nichman (leonid.nichman@manchester.ac.uk)

The copyright of individual parts of the supplement might differ from the CC-BY 3.0 licence.

1 **Supplementary materials**

2 **The CLOUD Chamber**

3 The CLOUD chamber is a 3 m-diameter electropolished stainless-steel cylinder (26.1 m^3). An
4 insulated thermal housing surrounds the chamber. The temperature is controlled by precisely
5 regulating the temperature of the air circulating in the space between the chamber and the
6 thermal housing. Experimental runs can be performed at highly stable temperatures (near
7 $0.01\text{ }^\circ\text{C}$) between $+40\text{ }^\circ\text{C}$ and $-70\text{ }^\circ\text{C}$. Ultra-pure synthetic air is obtained from the
8 evaporation of cryogenic liquid N_2 and liquid O_2 , mixed in the ratio 79:21 (Fig. S1),
9 respectively. The air is humidified using ultra-pure water from a filtered re-circulation
10 system. Ozone is added to the chamber by UV irradiation of a small inlet flow of dry air.
11 Magnetically coupled stainless steel fans on both manhole covers serve to mix the fresh gases
12 and beam ions, and ensure uniformity inside the chamber (Voigtlander et al., 2012). Volatile
13 trace gases such as SO_2 or NH_3 are supplied from concentrated gas cylinders pressurised with
14 N_2 carrier gas. The trace gas mixtures are highly diluted using synthetic air before injection
15 into the chamber. Less volatile trace gases such as alpha-pinene ($\text{C}_{10}\text{H}_{16}$) are supplied from
16 temperature-controlled stainless steel evaporators using ultrapure N_2 carrier gas. In order to
17 compensate for sampling losses, there is a continuous flow of fresh gases into the chamber of
18 about 150-250 L/min, resulting in a dilution lifetime of 2-3 h. The chamber and gas system
19 are designed to operate at pressure up to 123.3 kPa and to make controlled adiabatic
20 expansions down to 101.8 kPa. In this way, starting from relative humidity near 100 %, the
21 chamber can be operated as a classical Wilson cloud chamber for studies of ion-aerosol
22 interactions with cloud droplets and ice particles. The chamber can be evacuated from 121.3
23 kPa to 101.8 kPa over any chosen time interval above 10 sec, in order to simulate the
24 adiabatic cooling in ascending air masses that form clouds. Multistep programmed variations
25 of pressure drop are available for cloud lifetime extension or regrowth. Two 60 cm in
26 diameter fans rotating at speeds up to 400 RPM are responsible for uniform mixing in the
27 chamber. (For more details see Duplissy et al., 2015, and Kirkby et al., 2011)



1

2 Fig. S1 Simplified diagram of the CLOUD chamber.

3

1 Table S2. Lower and upper size bin thresholds in CASPOL.

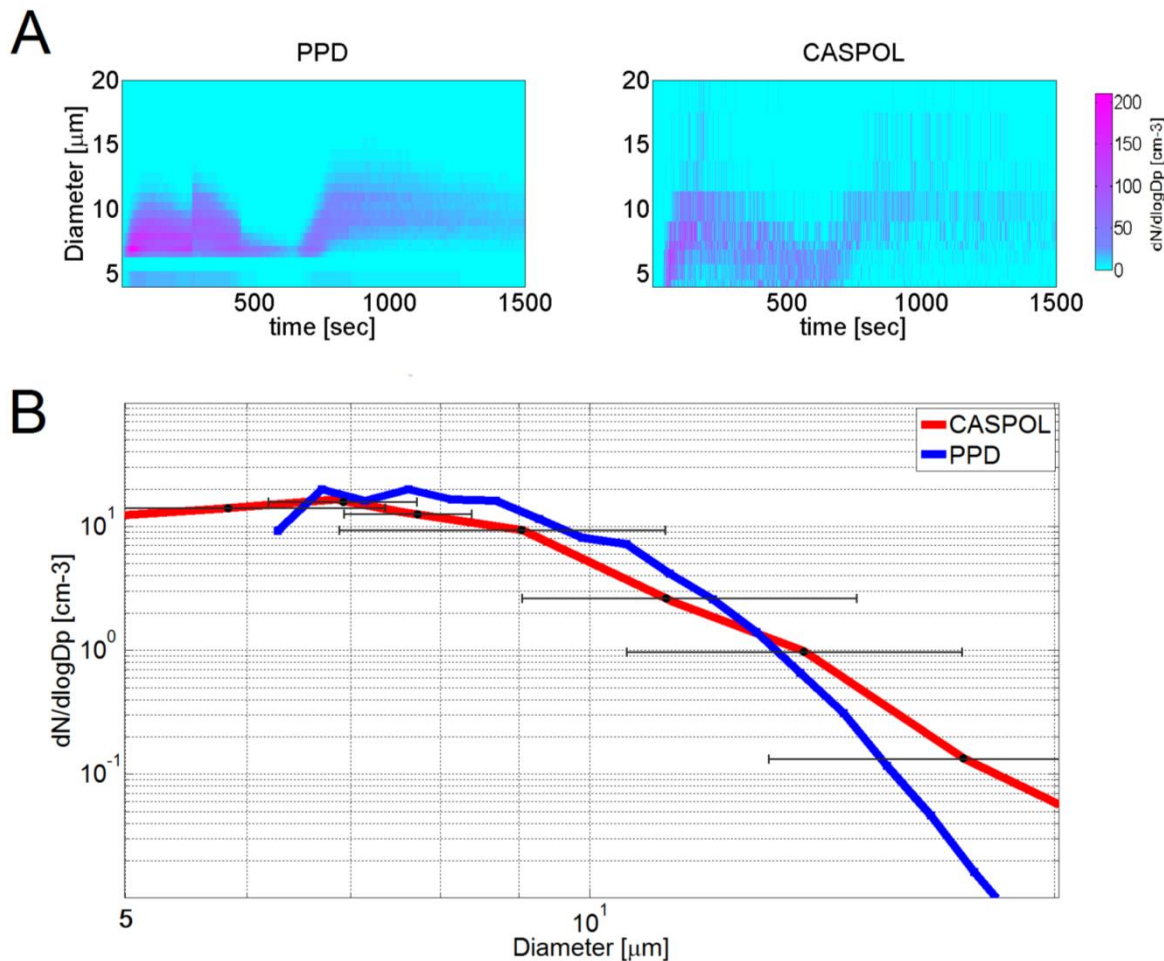
Bin number	Bin lower threshold	Bin upper threshold
1	0.51	0.61
2	0.61	0.68
3	0.68	0.75
4	0.75	0.82
5	0.82	0.89
6	0.89	0.96
7	0.96	1.03
8	1.03	1.10
9	1.10	1.17
10	1.17	1.25
11	1.25	1.5
12	1.5	2
13	2	2.5
14	2.5	3
15	3	3.5
16	3.5	4
17	4	5
18	5	6.5
19	6.5	7.2
20	7.2	7.9
21	7.9	10.2
22	10.2	12.5
23	12.5	15
24	15	20
25	20	25
26	25	30
27	30	35
28	35	40
29	40	45
30	45	50

2

1 Table S3. The intensities of the CASPOL detectors are amplified and digitized in stages: 3
 2 gain stages in the forward scattering direction and 2 in the backward. Signal to size
 3 conversion requires the adjusted linearly scaled reading of PBP data. Adjustments to the
 4 Forward, Backward and the Dpol signals are summarized.

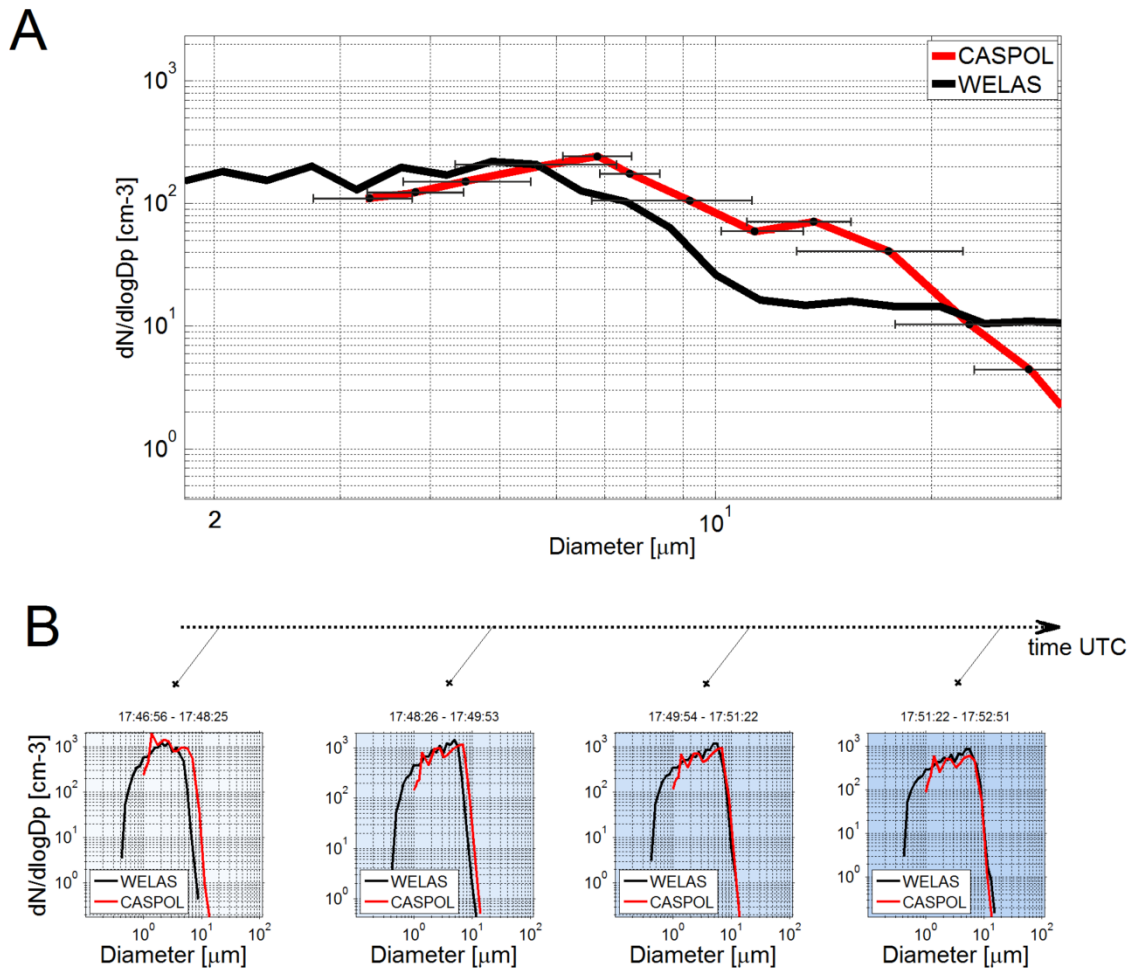
Forward Analog to Digital (A/D) counts	Adjusted Forward (A/D) counts
20 – 3071	20 – 3071
3072 – 6143	$([Forward\ Size] - 3071) \cdot 22 + 3072$
6143 – 9216	$([Forward\ Size] - 6143) \cdot 506 + (6143 - 3071) \cdot 22 + 3072$
Backward (A/D) counts	Adjusted Backward (A/D) counts
0 – 2000	0 – 2000
2001 – 3071	$([Backward\ Signal] - 2001) \cdot 22 + 2001$
Dpol (A/D) counts	Adjusted Dpol (A/D) counts
0 – 2730	0 – 2730
> 2730	$([Dpol\ signal] - 2731) \cdot 22 + 2731$

1
2



3

4 Figure S4. Ice measurements (-50°C) PPD-CASPOL comparison (Run # 1298.20),
5 Represented as ‘Ice - CLOUD 8’ in Fig. 8 (A) Particle Size Distribution (PSD) plots: PPD,
6 CASPOL. (B) Total PSD for the whole run.



1
2 Figure S5. Super-cooled water droplets (-10^0C) (Run # 1311.03). Represented as
3 ‘Supercooled, frozen droplets – CLOUD 8’ in Fig. 8 (A) CASPOL WELAS, total PSD
4 comparison for the whole run (B) Comparison of sequential time frames.
5

1 **References**

- 2 Duplissy, J., Merikanto, J., Franchin, A., Tsagkogeorgas, G., Kangasluoma, J., Wimmer, D.,
3 Vuollekoski, H., Schobesberger, S., Lehtipalo, K., Flagan, R., Brus, D., Donahue, N.,
4 Vehkämäki, H., Almeida, J., Amorim, A., Barmet, P., Bianchi, F., Breitenlechner, M.,
5 Dunne, E., Guida, R., Henschel, H., Junninen, H., Kirkby, J., Kürten, A., Kupc, A.,
6 Määttänen, A., Makhmutov, V., Mathot, S., Nieminen, T., Onnela, A., Praplan, A.,
7 Riccobono, F., Rondo, L., Steiner, G., Tome, A., Walther, H., Baltensperger, U., Carslaw, K.,
8 Dommen, J., Hansel, A., Petäjä, T., Sipilä, M., Stratmann, F., Vrtala, A., Wagner, P., Worsnop,
9 D., Curtius, J., and Kulmala, M.: Effect of ions on sulfuric acid-water binary particle
10 formation II: Experimental data and comparison with QC-normalized classical nucleation
11 theory, *J. Geophys. Res.-Atmos.*, doi: 10.1002/2015JD023539, 2016.

12 Kirkby, J., Curtius, J., Almeida, J., Dunne, E., Duplissy, J., Ehrhart, S., Franchin, A., Gagne,
13 S., Ickes, L., Kurten, A., Kupc, A., Metzger, A., Riccobono, F., Rondo, L., Schobesberger, S.,
14 Tsagkogeorgas, G., Wimmer, D., Amorim, A., Bianchi, F., Breitenlechner, M., David, A.,
15 Dommen, J., Downard, A., Ehn, M., Flagan, R. C., Haider, S., Hansel, A., Hauser, D., Jud,
16 W., Junninen, H., Kreissl, F., Kvashin, A., Laaksonen, A., Lehtipalo, K., Lima, J., Lovejoy,
17 E. R., Makhmutov, V., Mathot, S., Mikkila, J., Minginette, P., Mogo, S., Nieminen, T.,
18 Onnela, A., Pereira, P., Petaja, T., Schnitzhofer, R., Seinfeld, J. H., Sipila, M., Stozhkov, Y.,
19 Stratmann, F., Tome, A., Vanhanen, J., Viisanen, Y., Vrtala, A., Wagner, P. E., Walther, H.,
20 Weingartner, E., Wex, H., Winkler, P. M., Carslaw, K. S., Worsnop, D. R., Baltensperger, U.,
21 and Kulmala, M.: Role of sulphuric acid, ammonia and galactic cosmic rays in atmospheric
22 aerosol nucleation, Nature, 476, 429-433,
23 <http://www.nature.com/nature/journal/v476/n7361/abs/nature10343.html#supplementary-information>, 2011.

25 Voigtländer, J., Duplissy, J., Rondo, L., Kürten, A., and Stratmann, F.: Numerical simulations
26 of mixing conditions and aerosol dynamics in the CERN CLOUD chamber, *Atmos. Chem.*
27 *Phys.*, 12, 2205-2214, doi:10.5194/acp-12-2205-2012, 2012.
28